Available online at www.sciencedirect.com
ScienceDirect
Journal of Solid State Chemistry 180 (2007) 2534–2540
JOURNAL OF SOLID STATE CHEMISTRY
www.elsevier.com/locate/jssc

Copper–indium ordering in $RECu_6In_6$ (RE = Y, Ce, Pr, Nd, Gd, Tb, Dy)

Roman Zaremba[a], Ihor Muts[a,b], Rolf-Dieter Hoffmann[a], Yaroslav M. Kalychak[b], Vasyl' I. Zaremba[b], Rainer Pöttgen[a,*]

[a]*Institut für Anorganische und Analytische Chemie, Universität Münster, Corrensstrasse 30, 48149 Münster, Germany*
[b]*Inorganic Chemistry Department, Ivan Franko National University of Lviv, Kyryla and Mephodiya Street 6, 79005 Lviv, Ukraine*

Received 10 April 2007; received in revised form 19 June 2007; accepted 30 June 2007
Available online 7 July 2007

Abstract

The rare earth metal–copper–indides $RECu_6In_6$ (RE = Y, Ce, Pr, Nd, Gd, Tb, Dy) were synthesized from the elements by arc-melting. Well-crystallized samples were obtained by slowly cooling the melted buttons from 1320 to 670 K in sealed silica tubes in a muffle furnace. They were investigated by X-ray diffraction on powders and single crystals: $ThMn_{12}$ type, space group $I4/mmm$, $Z = 2$, $a = 916.3(2)$, $c = 535.8(2)$ pm, w$R_2 = 0.063$, 216 F^2 values, 15 variables for YCu_6In_6, $a = 926.5(4)$, $c = 543.5(3)$ pm, w$R_2 = 0.064$, 314 F^2 values, 15 variables for $CeCu_6In_6$, $a = 925.7(4)$, $c = 540.1(3)$ pm, w$R_2 = 0.075$, 219 F^2 values, 15 variables for $PrCu_6In_6$, $a = 923.1(4)$, $c = 540.3(3)$ pm, w$R_2 = 0.071$, 218 F^2 values, 15 variables for $NdCu_6In_6$, $a = 917.7(4)$, $c = 540.2(3)$ pm, w$R_2 = 0.076$, 207 F^2 values, 15 variables for $GdCu_6In_6$, $a = 917.0(5)$, $c = 540.5(4)$ pm, w$R_2 = 0.062$, 215 F^2 values, 15 variables for $TbCu_6In_6$, $a = 915.2(8)$, $c = 540.7(7)$ pm, w$R_2 = 0.108$, 218 F^2 values, 15 variables for $DyCu_6In_6$. The structures have been refined with a split position (50% Cu + 50% In) for the 8j site. They can be explained by a tetragonal body-centered packing of CN 20 polyhedra (10Cu + 10In) around the rare earth atoms. The ordering models of the copper and indium atoms and the limitations/resolution of X-ray diffraction for this topic are discussed.

Keywords: Indides; Intermetallics; Crystal chemistry

1. Introduction

Except scandium, the rare earth metal (RE)–copper–indium systems have been thoroughly investigated in the last 30 years and the isothermal sections of the respective phase diagrams at 670 and 870 K (depending on the rare earth metal content) have been constructed. An overview on the crystal chemistry and physical properties of the many $RE_xCu_yIn_z$ phases is given in a recent review article [1].

So far more than 100 ternary compounds have been reported for these ternary systems, but only few of them have completely been characterized on the basis of single crystal diffractometer data. The series of $RECu_{5.1}In_{6.9}$ (RE = Y, Ce, Pr, Nd, Sm, Gd–Lu) [2,3] indides crystallizes with the tetragonal $ThMn_{12}$ type structure [4], space group $I4/mmm$. So far, several other series with compositions RET_4X_8 (T = late transition metal; X = element of the 3rd main group), RET_5X_7, RET_6X_6, and $RET_{10}X_2$ have been reported [5]. With respect to composition, several of them have no possibility for T–X ordering. Keeping the high tetragonal space group symmetry, a fully ordered structure is possible only for the composition RET_4X_8. When lowering the space group symmetry from $I4/mmm$ via a *translationengleiche* symmetry reduction of index 2 ($t2$) to $Immm$, an ordered composition RET_6X_6 is possible through splitting of the 8j subcell site into the fourfold sites 4f and 4h. This kind of ordering is realized for the series of $REFe_6Ga_6$ gallides [6] and has first been observed for $ScFe_6Ga_6$, $ZrFe_6Ga_6$, and $HfFe_6Ga_6$ [7].

Refinement of the $ErCu_{5.1}In_{6.9}$ structure on the basis of X-ray powder data revealed the following site occupancies:

*Corresponding author. Fax: +49 251 83 36002.
E-mail addresses: kalychak@franko.lviv.ua (Y.M. Kalychak), pottgen@uni-muenster.de (R. Pöttgen).

0022-4596/$ - see front matter © 2007 Elsevier Inc. All rights reserved.
doi:10.1016/j.jssc.2007.06.029

the rare earth atoms on the 2*a* site, In on 8*i*, and the mixed occupied sites 8*f* ($Cu_{0.85}In_{0.15}$) and 8*j* ($Cu_{0.422}In_{0.578}$) [3]. Since the composition of these indides is close to RET_6X_6, we were interested in the precise Cu/In ordering. The crystal growth and single crystal structure refinements of $RECu_6In_6$ (*RE* = Y, Ce, Pr, Nd, Gd, Tb, Dy) indides are reported herein.

2. Experimental

2.1. Synthesis

Starting materials for the preparation of the $RECu_6In_6$ (*RE* = Y, Ce, Pr, Nd, Gd, Tb, Dy) indides were ingots of the rare earth elements (Johnson Matthey, Chempur or Kelpin), copper wire (Johnson Matthey, ∅ 1 mm), and indium tear drops (Merck), all with stated purities better than 99.9%. The rare earth metal pieces were first arc-melted [8] to small buttons under ca. 600 mbar argon atmosphere. The argon was purified over titanium sponge (900 K), silica gel, and molecular sieves. The rare earth metal buttons were then mixed with pieces of the copper wire and the indium tear drops in the 1:6:6 atomic ratios and the mixtures were reacted in the arc-furnace and remelted three times to ensure homogeneity. The weight losses after the arc-melting procedures were always less than 0.5%. The light gray polycrystalline samples are brittle and stable in air over months. Finely ground powders are dark gray and single crystals exhibit metallic luster. For crystal growth, the arc-melted buttons were sealed in evacuated silica tubes and first rapidly heated at 1320 K in a muffle furnace. The temperature was then lowered at a rate of 5 K/h to 1020 K and then at a rate of 15 K/h to 670 K. The polycrystalline samples are stable in moist air over months.

2.2. X-ray powder data

The $RECu_6In_6$ samples were characterized through Guinier powder patterns using Cu$K\alpha_1$ radiation and α-quartz ($a = 491.30$, $c = 540.46$ pm) as an internal standard. The Guinier camera was equipped with an imaging plate system (Fujifilm, BAS-1800). The tetragonal lattice parameters (Table 1) were refined by least-squares calculations using the WinXPow software supplied by Stoe. To ensure correct indexing, the experimental patterns were compared with calculated ones [9], taking the atomic sites obtained from the structure refinements.

Table 1
Lattice parameters (Guinier powder data) of the ternary indium compounds $RECu_6In_6$ (*RE* = Y, Ce, Pr, Nd, Gd, Tb, Dy)

Compound	*a* (pm)	*c* (pm)	*V* (nm^3)
YCu_6In_6	916.3(2)	535.8(2)	0.4499
$CeCu_6In_6$	926.5(4)	543.5(3)	0.4665
$PrCu_6In_6$	925.7(4)	540.1(3)	0.4628
$NdCu_6In_6$	923.1(4)	540.3(3)	0.4604
$GdCu_6In_6$	917.7(4)	540.2(3)	0.4549
$TbCu_6In_6$	917.0(5)	540.5(4)	0.4545
$DyCu_6In_6$	915.2(8)	540.7(7)	0.4529

2.3. Single crystal X-ray diffraction

Irregularly shaped crystals of $RECu_6In_6$ (*RE* = Y, Ce, Pr, Nd, Gd, Tb, Dy) were selected from the crushed annealed samples. These crystals were glued to small quartz fibres using bees wax and first checked by Laue photographs on a Buerger camera, equipped with the same Fujifilm, BAS-1800 imaging plate technique. Good quality crystal of $CeCu_6In_6$, $PrCu_6In_6$, $GdCu_6In_6$, and $TbCu_6In_6$ were used for the intensity data collection on a Stoe IPDS II diffractometer (graphite monochromatized Mo$K\alpha$ radiation; oscillation mode). Numerical absorption corrections were applied to the data sets. The YCu_6In_6, $NdCu_6In_6$, and $DyCu_6In_6$ crystals were measured at room temperature by use of a four-circle diffractometer (CAD4) with graphite monochromatized Mo$K\alpha$ radiation and a scintillation counter with pulse height discrimination. Scans were taken in the $\omega/2\theta$ mode. Empirical absorption corrections were applied on the basis of Ψ-scan data, accompanied by spherical absorption corrections. Relevant crystallographic data for the data collections and evaluations are listed in Tables 2 and 3.

2.4. Scanning electron microscopy

The single crystals investigated on the diffractometer were analyzed using a Leica 420 I scanning electron microscope with CeO_2, the rare earth trifluorides, Cu, and InAs as standards. No impurity elements heavier than sodium were observed. The compositions determined by EDX (10±2 at% Y:45±2 at% Cu:45±2 at% In, 8±2 at% Ce:45±2 at% Cu:47±2 at% In, 8±2 at% Pr:44±2 at% Cu:48±2 at% In, 8±2 at% Nd:45±2 at% Cu:47±2 at% In, 8±2 at% Gd:47±2 at% Cu:45±2 at% In, 7±2 at% Tb:46±2 at% Cu:47±2 at% In, 8±2 at% Dy:47±2 at% Cu:45±2 at% In) are close to the ideal composition, i.e. 7.6:46.2:46.2. The standard uncertainties account for the analyses at various points (between 3 and 10 points per sample).

3. Results and discussion

3.1. Structure refinements

Careful analyses of the IDPS data sets revealed high Laue symmetry and body-centered tetragonal cells. There were no further systematic extinctions, leading to the space groups $I4/mmm$, $I4mm$, $I\bar{4}2m$, $I\bar{4}m2$ and $I422$, of which the centrosymmetric group was found to be correct during structure refinement. The atomic positions of $ErCu_{5.1}In_{6.9}$ [3] were taken as starting values and the seven structures were refined with anisotropic displacement parameters for

Table 2
Crystal data and structure refinement for YCu_6In_6, $CeCu_6In_6$, $PrCu_6In_6$, and $NdCu_6In_6$, space group $I4/mmm$, $Z = 2$

Empirical formula	YCu_6In_6	$CeCu_6In_6$	$PrCu_6In_6$	$NdCu_6In_6$
Molar mass	1159.07 g/mol	1210.28 g/mol	1211.07 g/mol	1214.40 g/mol
Unit cell dimensions	Table 1	Table 1	Table 1	Table 1
Calculated density	8.56 g/cm^3	8.62 g/cm^3	8.69 g/cm^3	8.76 g/cm^3
Crystal size	$30 \times 40 \times 190$ μm^3	$10 \times 30 \times 100$ μm^3	$40 \times 70 \times 120$ μm^3	$20 \times 40 \times 170$ μm^3
Detector distance	–	60 mm	60 mm	–
Exposure time	–	5 min	5 min	–
ω range; increment	–	0–180°; 1.0°	0–180°; 1.0°	–
Integr. param. A, B, EMS	–	13.0; 3.0; 0.014	13.5; 3.5; 0.012	–
Transm. ratio (max/min)	1.57	2.21	1.96	7.03
Absorption coefficient	35.2 mm^{-1}	32.6 mm^{-1}	33.2 mm^{-1}	33.7 mm^{-1}
$F(0\,0\,0)$	1014	1052	1054	1056
θ range	3–30°	3–35°	3–30°	3–30°
Range in $h\,k\,l$	±12, ±12, +7	±14, ±14, ±8	±12, ±12, ±7	±12, ±12, ±7
Total no. reflections	1435	3513	2413	2634
Independent reflections	216 ($R_{int} = 0.034$)	314 ($R_{int} = 0.038$)	219 ($R_{int} = 0.062$)	218 ($R_{int} = 0.081$)
Reflections with $I > 2\sigma(I)$	204 ($R_\sigma = 0.015$)	236 ($R_\sigma = 0.043$)	207 ($R_\sigma = 0.025$)	213 ($R_\sigma = 0.027$)
Data/parameters	216/15	314/15	219/15	218/15
Goodness-of-fit on F^2	1.179	0.966	1.154	1.279
Final R indices [$I > 2\sigma(I)$]	$R_1 = 0.028$	$R_1 = 0.028$	$R_1 = 0.034$	$R_1 = 0.029$
	w$R_2 = 0.062$	w$R_2 = 0.062$	w$R_2 = 0.073$	w$R_2 = 0.071$
R indices (all data)	$R1 = 0.029$	$R1 = 0.042$	$R1 = 0.036$	$R1 = 0.029$
	w$R_2 = 0.063$	w$R_2 = 0.064$	w$R_2 = 0.075$	w$R_2 = 0.071$
Extinction coefficient	0.0103(6)	0.0088(5)	0.023(2)	0.0063(5)
Largest diff. peak and hole	3.51/–2.92 e/Å^3	4.77/–2.47 e/Å^3	3.09/–2.62 e/Å^3	3.14/–2.93 e/Å^3

Table 3
Crystal data and structure refinement for $GdCu_6In_6$, $TbCu_6In_6$, and $DyCu_6In_6$, space group $I4/mmm$, $Z = 2$

Empirical formula	$GdCu_6In_6$	$TbCu_6In_6$	$DyCu_6In_6$
Molar mass	1227.41 g/mol	1229.08 g/mol	1232.66 g/mol
Unit cell dimensions	Table 1	Table 1	Table 1
Calculated density	8.96 g/cm^3	8.98 g/cm^3	9.04 g/cm^3
Crystal size	$10 \times 40 \times 50$ μm^3	$20 \times 40 \times 190$ μm^3	$20 \times 40 \times 60$ μm^3
Detector distance	60 mm	60 mm	–
Exposure time	25 min	8 min	–
ω range; increment	0–180°; 1.0°	0–180°; 1.0°	–
Integr. param. A, B, EMS	14.0; 4.0; 0.038	14.0; 4.0; 0.022	–
Transm. ratio (max/min)	1.94	4.68	2.89
Absorption coefficient	35.7 mm^{-1}	36.2 mm^{-1}	36.8 mm^{-1}
$F(0\,0\,0)$	1064	1066	1068
θ range	2–30°	3–30°	3–30°
Range in $h\,k\,l$	±12, ±12, ±7	±12, ±12, ±7	±12, ±12, ±7
Total no. reflections	1691	2303	2634
Independent reflections	207 ($R_{int} = 0.066$)	215 ($R_{int} = 0.031$)	218 ($R_{int} = 0.065$)
Reflections with $I > 2\sigma(I)$	175 ($R_\sigma = 0.033$)	212 ($R_\sigma = 0.013$)	205 ($R_\sigma = 0.028$)
Data/parameters	207/15	215/15	218/15
Goodness-of-fit on F^2	1.174	1.172	1.149
Final R indices [$I > 2\sigma(I)$]	$R_1 = 0.035$	$R_1 = 0.030$	$R_1 = 0.045$
	w$R_2 = 0.073$	w$R_2 = 0.062$	w$R_2 = 0.104$
R indices (all data)	$R1 = 0.044$	$R1 = 0.031$	$R1 = 0.048$
	w$R_2 = 0.076$	w$R_2 = 0.062$	w$R_2 = 0.108$
Extinction coefficient	0.0020(4)	0.0096(6)	0.013(1)
Largest diff. peak and hole	4.14/–3.30 e/Å^3	4.61/–3.66 e/Å^3	4.82/–3.92 e/Å^3

all atoms with SHELXL-97 (full-matrix least-squares on F_o^2) [10]. Refinement of the occupancy parameters revealed full occupancy of the 8*f* and 8*i* sites with copper and indium, respectively. In contrast, the 8*j* sites revealed an occupancy by ca. 50% copper and 50% indium and extremely anisotropic displacement parameters U_{11}

(ca. five times larger than U_{22}). Since copper (117 pm) and indium (150 pm) have different covalent radii [11], the extreme anisotropic displacement is a clear hint of copper–indium ordering. Since we observed half occupancy by copper and indium on the 8*j* sites, a subgroup with a splitting into two fourfold sites could solve the problem. This splitting is only possible in space group *Immm* [12], a *translationengleiche* subgroup of index 2 (*t*2) of *I*4/*mmm*. Consequently we refined all data sets in this lower symmetry space group, also accounting for twinning (010, 100, 00−1) due to the *translationengleiche* symmetry reduction. All data sets revealed batch scale factors of 0.5 within one standard deviation and fully occupied sites, but the anisotropic displacements were not well resolved. The copper site still had a high U_{22} parameter, while the U_{22} and U_{33} parameters of indium refined to zero. Furthermore, we observed non-negligible positive and negative residual densities in the final Fourier maps. This readily indicated too small domain sizes, although the samples were very slowly cooled down to 670 K. Thus, we observe no amplitude but phase addition. Consequently, we refined the structures with a split model with Cu/In statistics (50/50) and equal (constrained) isotropic displacement parameters. The refinements then smoothly converged to the residuals listed in Tables 2 and 3. The crystal chemical consequences and reasons for this behavior are discussed in the following section. Final difference Fourier syntheses revealed no significant residual peaks. The atomic parameters and interatomic distances are listed in Tables 4

Table 4
Atomic coordinates and isotropic displacement parameters (pm^2) of $RECu_6In_6$ (RE = Y, Ce, Pr, Nd, Gd, Tb, Dy)

Atom	Wyckoff site	*x*	*y*	*z*	U_{eq}
YCu_6In_6					
Y	2*a*	0	0	0	121(5)
Cu	8*f*	1/4	1/4	1/4	121(4)
In	8*i*	0.34049(9)	0	0	125(3)
*M*1[a]	8*j*	0.2776(3)	1/2	0	113(4)
*M*2[a]	8*j*	0.3170(3)	1/2	0	113
$CeCu_6In_6$					
Ce	2*a*	0	0	0	42(3)
Cu	8*f*	1/4	1/4	1/4	85(3)
In	8*i*	0.34226(8)	0	0	97(2)
*M*1[a]	8*j*	0.2779(2)	1/2	0	62(3)
*M*2[a]	8*j*	0.3105(2)	1/2	0	62
$PrCu_6In_6$					
Pr	2*a*	0	0	0	46(4)
Cu	8*f*	1/4	1/4	1/4	83(4)
In	8*i*	0.34213(9)	0	0	94(4)
*M*1[a]	8*j*	0.2777(3)	1/2	0	63(4)
*M*2[a]	8*j*	0.3115(3)	1/2	0	63
$NdCu_6In_6$					
Nd	2*a*	0	0	0	66(4)
Cu	8*f*	1/4	1/4	1/4	100(4)
In	8*i*	0.3417(1)	0	0	110(4)
*M*1[a]	8*j*	0.2783(3)	1/2	0	89(4)
*M*2[a]	8*j*	0.3119(3)	1/2	0	89
$GdCu_6In_6$					
Gd	2*a*	0	0	0	83(5)
Cu	8*f*	1/4	1/4	1/4	117(5)
In	8*i*	0.3406(1)	0	0	122(4)
*M*1[a]	8*j*	0.2779(4)	1/2	0	93(5)
*M*2[a]	8*j*	0.3165(4)	1/2	0	93
$TbCu_6In_6$					
Tb	2*a*	0	0	0	91(4)
Cu	8*f*	1/4	1/4	1/4	117(4)
In	8*i*	0.3401(1)	0	0	121(4)
*M*1[a]	8*j*	0.2783(3)	1/2	0	99(4)
*M*2[a]	8*j*	0.3177(3)	1/2	0	99
$DyCu_6In_6$					
Dy	2*a*	0	0	0	90(6)
Cu	8*f*	1/4	1/4	1/4	117(6)
In	8*i*	0.3399(2)	0	0	114(5)
*M*1[a]	8*j*	0.2778(4)	1/2	0	89(6)
*M*2[a]	8*j*	0.3192(4)	1/2	0	89

U_{eq} is defined as one third of the trace of the orthogonalized U_{ij} tensor.
[a]The *M*1 and *M*2 sites are statistically occupied with 25% Cu and 25% In. These sites were refined with equal displacement parameters.

Table 5
Interatomic distances (pm), calculated with the powder lattice parameters of $CeCu_6In_6$

Ce	4	In1	317.1
	8	M2	323.5
	8	M1	340.9
	8	Cu1	354.6
In1	4	Cu1	281.8
	1	In1	292.3
	2	M1	293.7
	2	M1	296.1
	2	M2	306.4
	1	Ce	317.1
	2	M2	322.7
	4	In1	341.4
Cu1	4	M1	269.8
	2	Cu1	271.8
	4	M2	274.3
	4	In1	281.8
	2	Ce	354.6
M1	1	M2	[30.2]
	4	Cu1	269.8
	2	M2	270.5
	2	M1	291.0
	2	In1	293.7
	2	In1	296.1
	2	Ce	340.9
	1	M2	381.3
M2	1	M1	[30.2]
	2	M2	248.2
	2	M1	270.5
	4	Cu1	274.3
	2	In1	306.4
	2	In1	322.7
	2	Ce	323.5
	1	M2	351.1
	1	M1	381.3

All distances within the first coordination spheres are listed. Standard deviations are $\leqslant$ 0.2 pm. Note that the M positions have only partial occupancy (see Table 4).

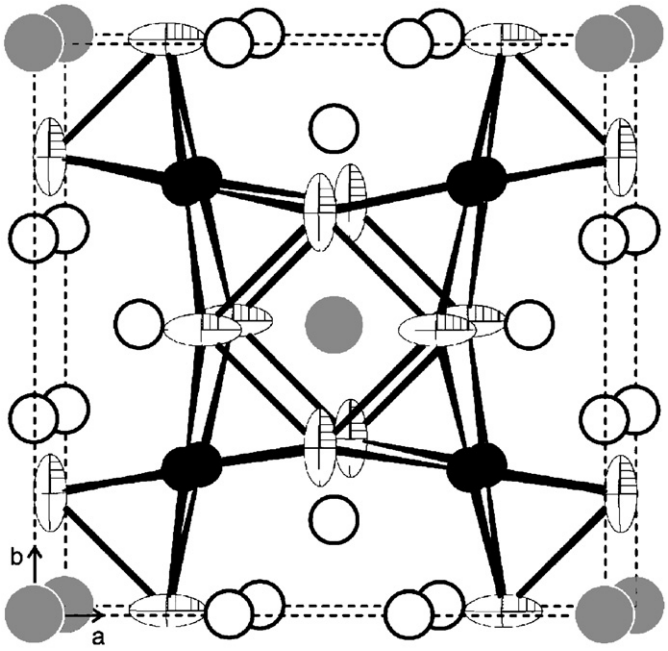

Fig. 1. The crystal structure of $CeCu_6In_6$. Cerium, copper, and indium atoms are drawn as medium gray, filled, and open circles, respectively. The copper–indium network around the cerium atoms is emphasized. The displacement ellipsoids of the mixed occupied Cu/In site are drawn at the 99% probability level.

and 5. Further data on the structure refinement are available.[1]

3.2. Crystal chemistry

The indides $RECu_6In_6$ (RE = Y, Ce, Pr, Nd, Gd, Tb, Dy) were structurally characterized on the basis of single crystal diffractometer data. Although we used very slow cooling rates down to 670 K, no long-range ordering of the copper and indium atoms was observed. The crystals had too small domain size, and consequently, the split model with Cu/In statistics was the best description for the investigated crystals. Nevertheless, we can assume a high degree of short-range order.

As a representative we present a view of the $CeCu_6In_6$ unit cell with the parameters obtained from the refinement without split positions in Fig. 1. Each cerium atom has coordination number (CN) 20 and the whole structure can be understood as a tetragonal body-centered packing of CN 20 polyhedra. In Fig. 2 the $xy0$ plane of this refinement result is shown. The elongated cigar-like shape of these $Cu_{0.5}In_{0.5}$ positions can be resolved in different ways. Keeping the high tetragonal symmetry, we can describe the structure only with Cu/In split positions with a

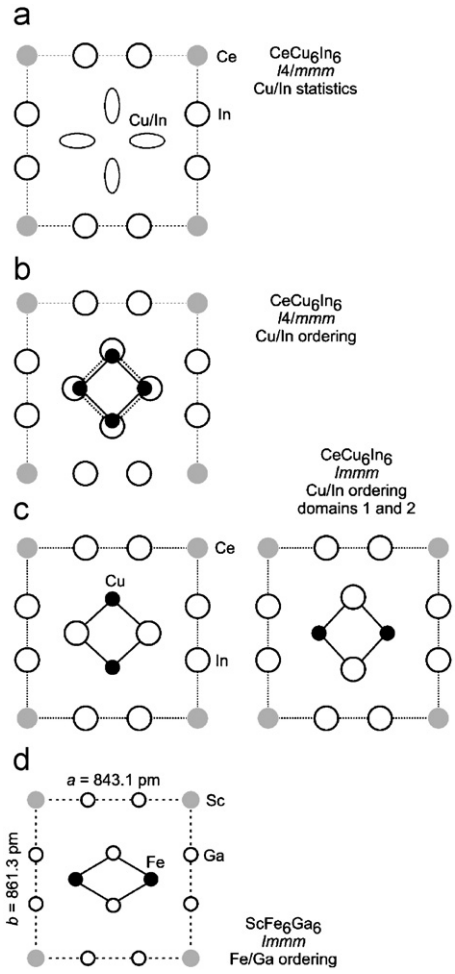

Fig. 2. View of the copper–indium network at $z = 0$ in the structure of $CeCu_6In_6$. Cerium, copper, and indium atoms are drawn as medium gray, filled, and open circles, respectively. The statistical model, a split model, and the different ordered models are presented together with the structure of $ScFe_6Ga_6$ [7]. For details see text.

statistical occupancy. This statistical model can be ordered in two ways: (i) an inner square uniquely occupied by copper and an outer one uniquely occupied by indium atoms or (ii) two Cu_2In_2 rhombs that are rotated by 90°. Since the split refinements clearly revealed full statistics, we can safely assume that the high symmetry model very well reproduces the overlap of the Cu_2In_2 rhombs rotated by 90°. This is a consequence of the twinning observed due to the *translationengleiche* symmetry reduction (the corresponding group–subgroup scheme is shown in Fig. 3). Refinement of the structures with the $Cu_{0.5}In_{0.5}$ cigars in all cases resulted in too small In–In distances in the range from 260 to 265 pm (depending on the size of the rare earth element). The split model presented here for the $RECu_6In_6$ indides has also been observed for the structure of $CaCu_{6.06}In_{5.94}$ [13]. A possible reason for the splitting is to allow the formation of suitable bond lengths between the copper and indium atoms. Similar split models also occurred for the $BaHg_{11}$-related phases $Y_3TaNi_{6+x}Al_{26}$ [14] and $M_3Au_{6+x}Al_{26}Ti$ (M = Ca, Sr, Yb) [15].

[1]Details may be obtained from: Fachinformationszentrum Karlsruhe, D-76344 Eggenstein-Leopoldshafen (Germany), by quoting the Registry Nos. CSD–391410 (YCu_6In_6), CSD–391411 ($CeCu_6In_6$), CSD–391412 ($PrCu_6In_6$), CSD–391413 ($NdCu_6In_6$), CSD–391419 ($GdCu_6In_6$), CSD–391420 ($TbCu_6In_6$), CSD–391421 ($DyCu_6In_6$).

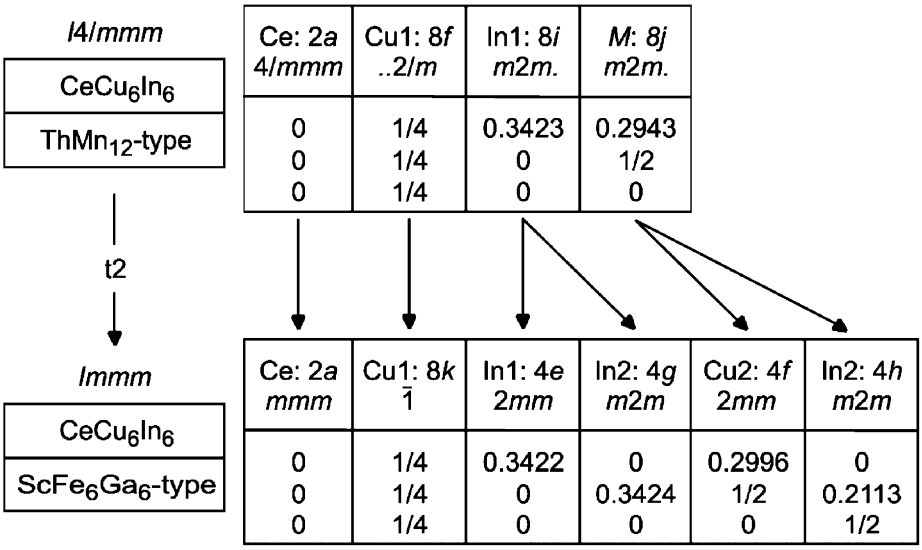

Fig. 3. Group–subgroup relation between the structures of $ThMn_{12}$ and $ScFe_6Ga_6$ in the *Bärnighausen* formalism [20,21]. The index of the *translationengleiche* symmetry reduction and the evolution of the atomic parameters are also given. For details see text.

The model with the fully ordered Cu_2In_2 rhombs corresponds to the $ScFe_6Ga_6$ type [7], space group *Immm*; however, there is a severe difference between this gallide and the indides reported herein. The *a* (843.1 pm) and *b* (861.3 pm) lattice parameters of $ScFe_6Ga_6$ [7] clearly show a strong orthorhombic distortion, similar to the series of the $REFe_6Ga_6$ gallides with the heavier rare earth elements [6]. For the $RECu_6In_6$ indides, neither the arc-melted nor the annealed samples gave indication for splitting of reflections in the powder patterns. Thus, we have no hint for an orthorhombic distortion. As already shown for the series of $REFe_6Ga_6$ gallides, formation of the superstructure is a function of the size of the rare earth element and temperature as well. For the indides the $[Cu_6In_6]$ network is much larger than the $[Fe_6Ga_6]$ network and this is most likely the reason that we still observe the tetragonal cell parameters for the indides.

From the refinement in space group *Immm* (ordered model) we can calculate the Cu–Cu, Cu–In, and In–In distances (as an example for the cerium compound) within the $[Cu_6In_6]$ network. The Cu–Cu distances of 272 pm are slightly longer than in *fcc* copper (256 pm) [16]. The various Cu–In distances range from 270 to 282 pm, close to the sum of the covalent radii of 267 pm [11]. The shortest In–In distances (291–313 pm) are all shorter than in tetragonal body-centered indium (4×325 and 8×338 pm) [16]. Similar short In–In distances occur in most indium rich $RE_xT_yIn_z$ compounds, e.g. the series $RE_4Pt_{10}In_{21}$ [17] or HT-GdNiIn$_2$ [18]. We can thus assume significant Cu–In and In–In besides weaker Cu–Cu bonding in these $RECu_6In_6$ indides.

The indides $REAg_6In_6$ (RE = La, Ce, Pr, Nd, Sm, Eu) [19] show similar $ThMn_{12}$-related unit cells. Precise single crystal studies with Ag$K\alpha$ radiation (since silver and indium differ by only two electrons) are in progress in order to determine the silver–indium ordering.

Acknowledgments

We are grateful to Dipl.-Ing. U.Ch. Rodewald for the intensity data collections and to Dipl.-Chem. F.M. Schappacher for the work at the scanning electron microscope. This work was supported by the Deutsche Forschungsgemeinschaft. I.R.M. is indebted to the DAAD for a research stipend.

References

[1] Ya. M. Kalychak, V. I. Zaremba, R. Pöttgen, M. Lukachuk, R.-D. Hoffmann, Rare Earth-Transition Metal-Indides. In K. A. Gschneidner Jr., V. K. Pecharsky, J.-C. Bünzli, Handbook on the Physics and Chemistry of Rare Earths, Elsevier, Amsterdam, vol. 34, 2005 (Chapter 218).
[2] Ya.M. Kalychak, A.M. Bakar, Izv. VUZ. Tsvetn. Metall. 6 (1989) 106.
[3] L.V. Sysa, Ya.M. Kalychak, A.M. Bakar, V.M. Baranyak, Krystallografiya 34 (1989) 744.
[4] J.V. Florio, R.E. Rundle, A.I. Snow, Acta Crystallogr. 5 (1952) 449.
[5] W. Suski, The $ThMn_{12}$-type compounds of rare earths and actinides: structure, magnetic and related properties. In: K.A. Gschneidner Jr., L. Eyring, (Eds.), Handbook on the Physics and Chemistry of Rare Earths, vol. 22, Elsevier, Amsterdam, 1996 (Chapter 149).
[6] F. Weitzer, K. Hiebl, P. Rogl, Yu.N. Grin, J. Appl. Phys. 68 (1990) 3512.
[7] N.M. Belyavina, V.Ya. Markiv, Dopov. Akad. Nauk. Ukr. RSR Ser. B (1982) 30.
[8] R. Pöttgen, T. Gulden, A. Simon, GIT Labor Fachzeitschrift 43 (1999) 133.
[9] K. Yvon, W. Jeitschko, E. Parthé, J. Appl. Crystallogr. 10 (1977) 73.
[10] G.M. Sheldrick, SHELXL-97, Program for Crystal Structure Refinement, University of Göttingen, Germany, 1997.
[11] J. Emsley, The Elements, Oxford University Press, Oxford, 1999.
[12] H. Wondratschek, U. Müller, in: International Tables for Crystallography, vol. A1: Symmetry Relations between Space Groups, Kluwer Academic Publishers, Dordrecht, 2004.
[13] L.V. Sysa, Ya.M. Kalychak, Neorg. Mater. 30 (1994) 779.
[14] R.E. Gladyshevskii, K. Cenzual, J. Alloys Compd. 240 (1996) 266.
[15] S.E. Latturner, M.G. Kanatzidis, Inorg. Chem. 43 (2004) 2.

[16] J. Donohue, The Structures of the Elements, Wiley, New York, 1974.
[17] V.I. Zaremba, V. Hlukhyy, U. Ch. Rodewald, R. Pöttgen, Z. Anorg. Allg. Chem. 631 (2005) 1371.
[18] V.I. Zaremba, V. Hlukhyy, R. Pöttgen, Z. Anorg. Allg. Chem. 631 (2005) 327.
[19] L.V. Sysa, Visnyk Lviv University, Ser. Khim. 31 (1991) 15.
[20] H. Bärnighausen, Commun. Math. Chem. 9 (1980) 139.
[21] H. Bärnighausen, U. Müller, Symmetriebeziehungen zwischen den Raumgruppen als Hilfsmittel zur straffen Darstellung von Strukturzusammenhängen in der Kristallchemie, University of Karlsruhe and University/GH Kassel, Germany, 1996.